Research paper

BDNF-producing, amyloid β-specific CD4 T cells as targeted drug-delivery vehicles in Alzheimer's disease

Ekaterina Eremenko [a,b,c,d,1], Kritika Mittal [a,b,c,d,1], Omer Berner [a,b,c,d], Nikita Kamenetsky [a,b,c,d], Anna Nemirovsky [a,b,c,d], Yehezqel Elyahu [a,b,c,d], Alon Monsonego [a,b,c,d,*]

[a] The Shraga Segal Department of Microbiology, Immunology and Genetics, Faculty of Health Sciences, Ben-Gurion University of the Negev, Beer Sheva 84105, Israel
[b] Zlotowski Center for Neuroscience, Ben-Gurion University of the Negev, Beer Sheva 84105, Israel
[c] Regenerative Medicine and Stem Cell Research Center, Ben-Gurion University of the Negev, Beer Sheva 84105, Israel
[d] The National Institute of Biotechnology in the Negev, Ben-Gurion University of the Negev, Beer Sheva 84105, Israel

ARTICLE INFO

ABSTRACT

Background: The delivery of therapeutic proteins to selected sites within the central nervous system (CNS) parenchyma is a major challenge in the treatment of various neurodegenerative disorders. As brain-derived neurotrophic factor (BDNF) is reduced in the brain of people with Alzheimer's disease (AD) and its administration has shown promising therapeutic effects in mouse model of the disease, we generated a novel platform for T cell-based BDNF delivery into the brain parenchyma.
Methods: We generated amyloid beta-protein (Aβ)-specific CD4 T cells (Aβ-T cells), genetically engineered to express BDNF, and injected them intracerebroventricularly into the 5XFAD mouse model of AD.
Findings: The BDNF-secreting Aβ-T cells migrated efficiently to amyloid plaques, where they significantly increased the levels of BDNF, its receptor TrkB, and various synaptic proteins known to be reduced in AD. Furthermore, the injected mice demonstrated reduced levels of beta-secretase 1 (BACE1)—a protease essential in the cleavage process of the amyloid precursor protein—and ameliorated amyloid pathology and inflammation within the brain parenchyma.
Interpretation: A T cell-based delivery of proteins into the brain can serve as a platform to modulate neurotoxic inflammation and to promote neuronal repair in neurodegenerative diseases.
© 2019 The Authors. Published by Elsevier B.V. This is an open access article under the CC BY-NC-ND license (http://creativecommons.org/licenses/by-nc-nd/4.0/).

1. Introduction

The development and optimization of platforms for targeted drug delivery to and within the central nerve system (CNS) is one of the key challenges in the treatment of neurodegenerative disorders, primarily due to the need to cross the blood-brain barrier [1,2]. During the past decades, several strategies for protein delivery to the CNS were developed using cells, [1,3–6], viral vectors [7,8], nanoparticles [9], liposomes [10], and specific transporters that facilitate the entry of proteins into the brain [11]. Among these delivery systems, systems involving cell-based drug-delivery into the brain received considerable attention due to the ability of the cells to locally release efficacious doses of the protein of interest [5,6,12,13] and/or their ability to replace damaged neural cells and modulate inflammation [12,14].

In Alzheimer's disease (AD), the accumulation of amyloid beta-protein (Aβ) and of neurofibrillary tangles in the hippocampus and cortex [15–17] is accompanied by neurotoxic inflammation, progressive neuronal loss, and cognitive decline [18–23], which can be ameliorated by cytokines, chemokines, and neurotrophic factors [2,21,24–28]. However, to date, the effective delivery of such proteins into specific brain loci (e.g., amyloid plaques) is a significant limiting step in the development of efficacious therapies.

One factor whose delivery into specific brain loci can potentially be used to ameliorate AD-related pathology is BDNF: a ubiquitous neurotrophin that is involved in neuronal plasticity, synaptogenesis, and long-term potentiation [29]. Reduced levels of BDNF—and of its receptor, TrkB—are often associated with the degeneration of hippocampal and cortical neurons, both in people with AD [30–34] and in mouse models of the disease [35,36]. In line with these observations, increasing BDNF in the brain, either by expressing it through viruses [7,37]

Research in context

Evidence before this study

BDNF deficiency is associated with the progression of Alzheimer's disease. Intra-brain delivery of BDNF is a promising therapeutic approach.

Added value of this study

Aβ-specific T cells can deliver BDNF into the brain of an Alzheimer's disease mouse model, increase the levels of BDNF and TrkB receptor at specific pathological sites in the brain and modulate neurotoxic inflammation. This is a proof of concept that a T-cell–based delivery system can be used effectively to deploy biological factors at specific brain regions.

Implication of all the available evidence

Aβ-specific T cells can effectively migrate inside the brain parenchyma, modulate neuroinflammation, and ameliorate plaque pathology. Thus, they can serve as a multi-target delivery system of beneficial proteins into the brain.

or transplanted cells [3,26], results in marked neuroprotective effects in several animal models of AD. Thus, developing a cell-based therapy that can bypass the adverse effects and carcinogenic risks of other brain-delivery approaches, could serve as a novel therapeutic approach to the targeted delivery of BDNF into the brain and, specifically, into pathologic sites.

Here, we used CD4 T cells to deliver BDNF directly and specifically to Aβ plaques in the brain of 5XFAD mice (a well-established mouse model of AD). Following to our prevoius findings that intracerebroventricular (ICV)-injected CD4 T cells effectively migrate into the brain parenchyma and target Aβ plaques in mice [38], we generated Aβ-specific CD4 T cells (Aβ-T cells), transduced them to express BDNF, and ICV-injected them into the mice to determine whether the targeted delivery of BDNF to sites of amyloid pathology can ameliorate the disease process.

2. Materials and methods

2.1. Mice

Female and male wild-type (WT) C57BL/6 mice and 5XFAD transgenic (Tg) mice (Swedish K670N, M671L, Florida I716V, London V717I, and two mutations in the human presenilin-1 gene M146L and L286V; stock number 34840) were purchased from The Jackson Laboratory (Bar Harbor, ME). All surgical and experimental procedures were reviewed and approved by the Institutional Animal Care and Use Committee of Ben-Gurion University of the Negev.

2.2. Aβ-specific T cell line

Mice were immunized at 2 m of age by a footpad injection of Aβ1–42 (100 μg; GenScript, Piscataway, NJ) emulsified in CFA H37Ra (Difco, Detroit, MI). The Aβ1–42 peptide used for immunization was initially dissolved in a small volume of DMSO to enhance solubility and then diluted to 2 mg/ml in PBS. The peptide was emulsified with CFA to a final concentration of 1 mg/ml. Ten days later, popliteal, inguinal, and iliac lymph nodes were extracted and the cells were seeded (5×10^6 cells/ml in a 24-well culture dish) in a complete RPMI medium (10% FCS, 10 mM HEPES, 1 mM sodium pyruvate, 10 mM non-essential amino acids, 1% Pen/Strep/Nystatin, and 50 μM 2-ME) supplemented with 20 μg/ml Aβ1–42. Every other day thereafter, human rIL-2

(20 U/ml) in complete RPMI was added to the culture. Following the first week and every 2 w thereafter, T cells (10^5 T cells/ml) were re-stimulated with irradiated (6000 rad) splenocytes (5×10^6 cell/ml) in 24-well plates. For Th1 polarization, neutralizing anti–IL-4 (20 μg/ml, clone 11B11; BioLegend, San-Diego, CA) and recombinant mouse IL-12 (1 ng/ml; BioLegend) were added to the culture in the first three stimulations, at seeding, and then 2 d later.

2.3. Cytokine ELISA

T cells (2×10^4) and irradiated (6000 rad) antigen-presenting cells (APCs; 5×10^5 cells) were cultured in U-shaped 96-well–plate culture dishes in a complete RPMI medium, either with or without the Aβ1–42 peptide at increasing concentrations (0, 2 and 20 μg/ml). IL-2 and IL-4 were measured in supernatants after 24 h, IFN-γ and IL-10 were measured after 48 h, and IL-17A was measured after 72 h, using sandwich ELISA (BioLegend) according to the manufacturer's instructions. All samples were analyzed as duplicates.

2.4. BDNF cloning and retroviral transduction of Th1 cells

The BDNF gene and a T2A-GFP fusion DNA were cloned into the retroviral vector pMP-71-G-Pre (kindly provided by Prof. Wolfgang Uckert, Max-Delbrück-Center for Molecular Medicine, Berlin, Germany) [39]. Plasmids were amplified using Match1 bacteria (Invitrogen, Carlsbad, CA) and purified with a Maxiprep Plasmid DNA Kit (Invitrogen). The packaging cell line Platinum-E (Cell Biolabs, Inc., San Diego, CA, USA) was transfected in a 10-cm plate with 20 μg of plasmid DNA and 60 μl of PolyJet™ (SignaGen Laboratories, Gaithersburg, MD). After 16 h, the medium was replaced with 10 ml of an RPMI complete medium. After 24 h and 48 h, the retrovirus supernatant was collected and filtered through a 0.45-μm filter. Th1 cells were stimulated for 48 h at a density of 1×10^6 cells/ml with 25 ul of anti-CD3/anti-CD28 Dynabeads (Thermo Fisher Scientific Inc., Waltham, MA). The Th1 cells were spinoculated with the viral supernatant on retronectin-coated plates (12.5 μg/ml; TaKaRa Bio Europe SAS, St. Germain en Laye, France) at 1500 g for 90 min at 32 °C, supplemented with 80 units of IL-2 and 4 μg/ml protamine sulfate (Sigma-Aldrich, St. Louis, MO).

2.5. Cloning of TrkB-T2A and retroviral transduction of HEK293T cells

Mouse TrkB cDNA (Sino Biological Inc., China) was cloned in the pMP71 expression vector [39]. The packaging cell line Platinum-E was transfected in a 10-cm plate with 20 μg of plasmid DNA and 60 μl of a PolyJet™ transfection reagent. After 16 h, the medium was replaced with 10 ml of a DMEM medium supplemented with 10% FBS and 1% Pen/Strep/Nystatin. After 24 h and 48 h, the supernatant was collected, filtered through a 0.45-μm filter, and used to transduce human embryonic kidney cells (HEK293T) in the presence of 4 μg/ml protamine sulfate (Sigma-Aldrich). After 72 h, the GFP+ cells were analyzed using flow cytometry (CytoFLEX, configuration B5-R3-V5; Beckman Coulter, Brea, CA) and sorted using FACS Aria (BD Biosciences, San Jose, CA).

2.6. Intracerebroventricular injection of CD4 T cells

Resting CD4 T cells were re-stimulated with 25 μl of anti-CD3/anti-CD28 Dynabeads (Thermo Fisher Scientific Inc.) for 36 h. The cells were then harvested and resuspended in PBS at a concentration of 50,000 cells/μl. After anesthetizing the mice with 1.5% of isoflurane, 2.5×10^5 cells were slowly injected, over a period of 5 min, into each of the lateral ventricles of the brain using a stereotactic device [coordinates relative to bregma: latero-lateral (x) $= +1/-1$, dorso-ventral (y) $= -0.5$, rostro-caudal (z) $= -2.30$]. Control mice underwent the same procedure, but they were injected with PBS only (5 μl into each of the lateral ventricles).

2.7. Immunohistochemistry

Mice were killed with an overdose of isoflurane and perfused with cold PBS. Their brains were removed and immersed in a 4% paraformaldehyde solution in 4 °C overnight, transferred to a 30% sucrose solution in 4 °C for 48 h, and then fixed in OCT (Tissue-Tek, Torrance, CA). Sagittal sections (35 mm) of the brain were produced with a cryostat (Leica CM3050) and kept in −20 °C until used. Sections were rinsed twice in a washing solution (0.05% PBS/Tween 20) and permeabilized for 30 min in 0.5% PBS/Triton X-100. Prior to staining, a primary antibody diluting buffer (Biomeda, Foster City, CA) was used to block nonspecific binding. Fluorescently stained sections were examined under an Olympus Fluoview FV1000 laser-scanning confocal microscope (Olympus, Hamburg, Germany) and ZEISS Laser Scanning Microscope with Airyscan (Zeiss Microscopy GmBH, Gottingen, Germany).

2.7.1. CD4 T-cell quantification and co-localization with Aβ.

Sections (35 mm thick) were imaged under a confocal microscope and analyzed by using the IMARIS software. The software settings were optimized to identify only the immunolabeled CD4 T cells. Using the "Surface plug-in" option in IMARIS, the number of CD4+ T cells were calculated. To quantify co-localization, 3D reconstructions generated using the Surface plug-in were viewed in IMARISColoc, operated simultaneously on two channels, to measure the degree of overlap between the two channels. The intensity threshold of each channel was calculated by choosing the Automatic Threshold Calculation option. The overlap image was saved as a separated channel, which was then processed by using the Surface plug-in. To calculate the number of CD4 T cells co-localized with Aβ, "number of events" was divided by total volume of the imaged area. At least four sections were analyzed per brain.

2.7.2. Analysis of Aβ plaque load

A quantification analysis of Aβ plaque load in the cortex of the brain was performed in two sections (35 mm thick) per hemisphere immunolabeled for Aβ. Fluorescence intensity was first obtained in sections from control mice (injected with PBS) and identical laser-scanning parameters were then used for the entire experiment. Using the IMARIS image analysis software, an intensity threshold was set to mark only those areas showing significant staining. The average fluorescent area per brain section was calculated for each of the analyzed groups.

2.8. Western blotting

Cells were lysed in a RIPA buffer [50 mM Tris-Cl, pH 8.0, 150 mM NaCl, 1% Triton, 0.5% sodium dodecyl sulfate (SDS)] containing protease inhibitor cocktail p8340 (Sigma-Aldrich, St. Louis, MO), and phosphatase inhibitor cocktail C sc-45065 (Santa Cruz Biotechnology Inc., Texas, USA). Cell lysates (20–30 μg) were separated on 12% Tris-Glycine SDS-PAGE gels and then transferred to PVDF or nitrocellulose membranes. Mouse brains were homogenized in a TTB buffer containing a protease inhibitor cocktail (p8340, Sigma-Aldrich) and phosphatase inhibitor cocktails 2 and 3 (p0044, p5726, Sigma-Aldrich). One hemisphere was used for qPCR, and the other hemisphere was lysed in a RIPA buffer (using 1% NP-40 instead of Triton and 0.5% sodium deoxycolate) containing a protease inhibitor cocktail and phosphatase inhibitor cocktails 1 and 2. Next, 20–30 μg of lysate were separated in 10–15% Tris-Glycine SDS-PAGE gels, transferred to PVDF or nitrocellulose membranes, and blocked with 5% BSA Fraction V (Merck Millipore). The membranes were incubated overnight with the antibodies (see below) and WesternBright Quantum (Advansta Inc., San Jose, CA) was used to visualize the chemiluminescent signal. The images were captured using a bioimaging analyzer (Fusion-FX; Vilber, France) and analyzed using ImageJ software.

2.9. Antibodies and kits

2.9.1. Immunocytochemistry/immunohistochemistry

Purified rat anti-CD4 (201,501, 1:100) was purchased from BioLegend. Purified rabbit anti-BDNF (ANT-010; 1:100) was purchased from Alomone Labs LTD (Jerusalem, Israel). Rabbit anti-human Aβ antibodies (1:250) were generated at our animal facility and examined for specificity by ELISA and immunohistochemistry (IHC). Anti-pTrkB (pTyr[816]) and Anti-NeuN (MAB377) were purchased from Sigma-Aldrich (ABN1381). Anti-MAP2 (AB5622) was purchased from Merck Millipore. Alexa 488, 546, or 633 antibodies (Invitrogen), diluted 1:250–500, were used for secondary staining. TO-PRO-3 (Invitrogen) and DAPI (Thermo Fisher Scientific Inc.) were used for counterstaining.

2.9.2. Western blotting

The following antibodies were used for Western blot (WB) analyses were purchased from Cell Signaling: anti-Synaptophysin polyclonal (Cat. # 5461), anti-PSD95 polyclonal (Cat. # 2507), anti-phospho-TrkB (Tyr706/707) (Cat. # 4621), anti-TrkB (Cat. # 4603), anti-SNAP25 (Cat. # 5309), anti-β-tubulin (Cat. # 2128), anti-VAMP2 (Cat. # 13508), anti-BACE (Cat. # 5606), anti-p44/42 MAPK (Erk1/2) (Cat. # 4695) and anti-Phospho-p44/42 MAPK (Erk1/2) (Thr202/Tyr204) (Cat. # 4370). Anti-NeuN was purchased from Sigma-Aldrich (MAB377). Anti-vinculin antibody was purchased from Abcam (ab129002). Anti-actin was purchased from Merck Millipore (MAB1501).

2.9.3. Flow cytometry

The following antibodies were purchased from BioLegend: anti-CD45.2 (AF700, Cat. # 109,821), anti-CD4 (BV785, Cat. # 100453), anti-CD25 (APC-Cy7, Cat. # 102025), and anti-CD11b (BV+510, Cat. # 101245).

2.10. Quantitative PCR

Mice were perfused with PBS and half brains were immediately frozen in liquid nitrogen and stored at −80 °C. The brains were then homogenized in a TTB buffer containing a protease inhibitor cocktail and a phosphatase inhibitor cocktails. A TRI Reagent® (Sigma-Aldrich, St. Louis, MO) was added to the homogenized brains, RNA was extracted by a phenol-chloroform procedure, and RNA quality and quantity were examined by using the NanoDrop 1000 spectrophotometer (Thermo Fisher Scientific Inc). A total of 2 μg RNA was reverse-transcribed with a high-capacity cDNA reverse transcription kit (Thermo Fisher Scientific Inc.) and 20 ng of cDNA were used for qPCR analysis. Target gene-specific primer sequences and suitable probes were designed by the Universal Probe Library System software (Roche Molecular Systems, Inc. CA). CXXC1 was used as an endogenous control to normalize gene expression.

2.11. Flow cytometry

Mice were euthanized by isoflurane inhalation, perfused, and their brains were collected in cold PBS. The isolated brains were minced and digested for 1 h at 37 °C in Hanks' Balanced Salt Solution (HBSS) (02–017-1A, Biological Industries Israel Beit Haemek LTD, Israel) containing 50 μg/ml DNase I and 100 μg/ml collagenase (Roche, Rotkreuz, Switzerland). The resulting cell suspension was passed through a 70-μm Nylon mesh (Falcon, BD Biosciences, Bedford, MA), pelleted, resuspended in 30% Percoll (GE Healthcare Bio-Sciences, NJ) in HBSS and centrifuged at 15,500 rpm for 30 min at 4 °C. After eliminating the myelin debris, the mononuclear cell phase was collected. CNS-mononuclear cells were washed in a FACS buffer (HBSS, 2% FCS, 10 mM EDTA). After blocking non-specific binding of immunoglobulins to Fc receptors (anti-mouse CD16/32, TrueStain FcX TM, BioLegend), the cells were

Fig. 1.
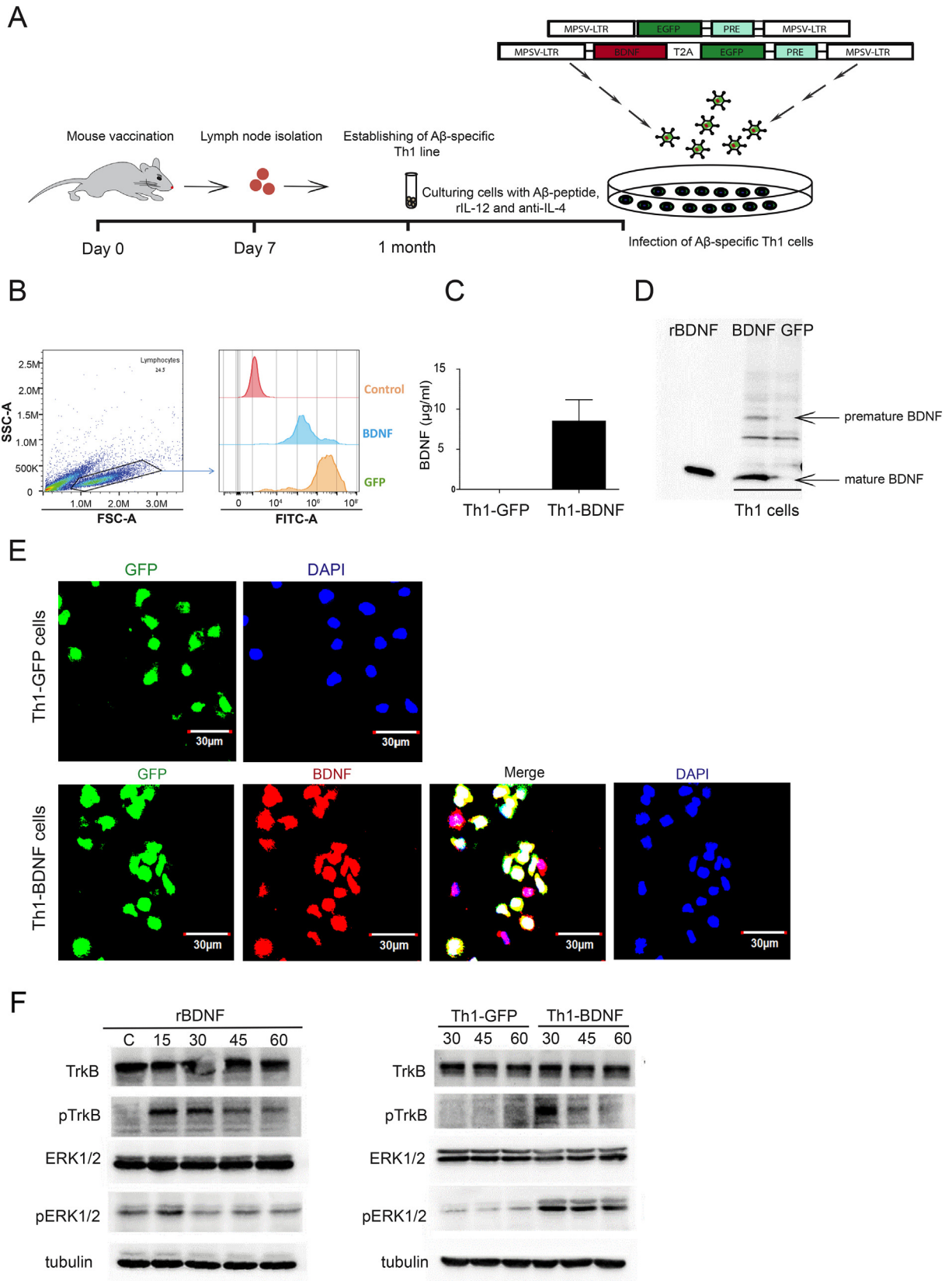
stained for 15 min at 4 °C with specific antibodies, washed, and analyzed. Multicolor FACS analyses were performed with a Cytoflex.

2.12. Isolation of primary hippocampal neurons and co-culturing with Aβ-specific T cells

Primary hippocampal neurons were isolated from newborn C57BL/6 pups as described [40] with minor modifications. Briefly, hippocampi were collected into HBSS buffer, dissociated with papain (Sigma-Aldrich, P3125) and then seeded in chambers (μ-slide 4-well glass bottom, IBIDI GmbH Martinsried, Germany, 80427) coated with poly-L-lysine (Sigma-Aldrich, P-0899), using Neurobasal medium (GIBCO, 21103–049), supplemented with B-27 (GIBCO, 17504044), GlutaMAX (GIBCO, 35050–061) and 2% FBS (HyClone). After 24 h, medium was replaced with a serum-free Neurobasal medium. At day 14, neurons were placed under starvation conditions for 4 h and were then incubated with Th1-GFP or Th1-BDNF cells (activated with anti-CD3/antiCD28 Dynabeads 24 h before the co-culture) for 2 h. Co-cultured cells were fixed with 2% PFA and immunolabeled with antibodies. Images were taken using ZEISS Laser Scanning Microscope 880 with Airyscan and analyzed using ZEN software.

2.13. Statistical analyses

All statistical analyses were performed with GraphPad Prism version 5.02 for Windows (GraphPad Software, San Diego, CA). All variables are expressed as means ± SEM, as indicated in figure legends. The p-values were calculated with an unpaired t-test or with a one-way ANOVA, as indicated in figure legends.

2.14. Ethics statement

The study was conducted in accordance with the recommendations of the 1994 law for the prevention of cruelty to the animals (experiments on animals). The protocol was approved by University Committee for the Ethical Care and Use of the Animals in Experiments, authorization number 45-07-2015.

3. Results

3.1. Generation of Aβ-specific Th1 cells transduced to overexpress BDNF

We first generated Aβ-specific CD4 T cells polarized to Th1, and transduced them to overexpress BDNF. Adult C57BL6 mice were immunized with Aβ1–42 and, 10 d later, lymph node-derived CD4 cells T cells were stimulated in the presence of Aβ1–42, APCs, and a Th1 polarizing cocktail (Fig. 1A). The T cells were then transduced with retroviruses pMP71G-PRE under the MPSV promotor [39] to express either BDNF and GFP (hereon termed Th1-BDNF) or GFP alone (hereon termed Th1-GFP) (Fig. 1A) and sorted to 95% purity (Fig. 1B). BDNF expression by Th1-BDNF cells was validated by ELISA, WB, and immunocytochemistry (ICC) (Fig. 1C–E). Forty-eight hours after the stimulation, Th1-BDNF, but not Th1-GFP cells, activated with anti-CD3/anti-CD28 Dynabeads, secreted 8.51 ± 3.8 ng/ml BDNF (Fig. 1C). The WB analysis indicated that both premature and mature forms of BDNF were expressed by the Th1-BDNF, and not by the Th1-GFP cells (Fig. 1D).

The expression of specific Th1 cytokines (e.g., IL-2, IFN-γ) was validated by ELISA (Supplementary Fig. 1). To test whether the secreted BDNF is functional, we transduced HEK293T cells to stably express the mouse BDNF receptor TrkB (HEK293T-TrkB) under the MPSV promoter. HEK293T-TrkB cells were then cultured with supernatants collected from bead-activated Th1-BDNF cells, Th1-GFP cells, or recombinant BDNF. As shown in Fig. 1F, incubating HEK293T-TrkB cells with recombinant BDNF or with supernatants from Th1-BDNF producing cells, but not with supernatants from Th1-GFP cells, resulted in TrkB and Erk1/2 phosphorylation, which was observed 15 min (recombinant BDNF) or 30 min (recombinant BDNF and Th1-BDNF supernatant) after the incubation (Fig. 1F). These data demonstrate that Th1-BDNF cells secrete a biologically active BDNF.

3.2. ICV-injected Th1-BDNF cells target amyloid plaques in the brain of 5XFAD mice

To determine whether Th1-BDNF cells infiltrate the brain parenchyma and migrate to brain regions loaded with amyloid plaques, 10–11 month old 5XFAD mice were ICV-injected with 0.25×10^6 Th1-BDNF or Th1-GFP cells, or with PBS, to each hemisphere. The mice were killed 10 d post injection (dpi), and one set of brain hemispheres was analyzed with flow cytometry or IHC while the other was analyzed with WB and qPCR (Fig. 2A). Fig. 2B shows flow cytometry analysis of brain mononuclear cells gated for CD11b−CD4+ and then for CD4+GFP+ cells. Whereas, CD4+GFP+ cells were not observed in 5XFAD mice ICV-injected with PBS, a significant fraction of CD4+GFP+ cells were observed among the mononuclear cells of 5XFAD mice ICV-injected with Th1-GFP or with Th1-BDNF cells (2.99 ± 2.59% and 6.87 ± 3.57%, respectively) (Fig. 2B). There were no significant differences in the frequency of GFP+ cells and their CD25 MFIs (as an indication for their state of activation) among the infiltrating CD4 T cells (Fig. 2B). Importantly, IHC analysis of brain sections immunolabeled with anti-Aβ, revealed that GFP+ T cells were distributed in areas deposited with Aβ plaques (Fig. 2C). To determine the amount of GFP+ T cells co-localized with Aβ plaques, we quantified the total number of T cells and the fraction that were co-localized with Aβ plaques at 10 and at 21 dpi. Whereas greater number of T cells were observed in the tissue at 10 dpi, a bigger fraction of the T cells were co-localized with Aβ plaques at 21 dpi (Fig. 2C). Immunolabeling with anti-BDNF and anti-CD4 shows that the ICV-injected Th1-BDNF cells maintained the expression of GFP and BDNF within the brain parenchyma (Fig. 2D). We thus demonstrate that both Th1-GFP or Th1-BDNF cells ICV-injected to 5XFAD mice effectively migrate toward amyloid plaques and express the activation marker CD25. Furthermore, the Th1-BDNF cells were co-localized with BDNF within the brain parenchyma, indicating that the migration process does not affect its active expression.

3.3. ICV-injected Th1-BDNF cells enhance neuronal repair in 5XFAD mice

AD is characterized by region-specific BDNF imbalances in the brain, especially in the hippocampus and cortex [27,31,41]. We thus determined the levels of BDNF–and its receptor TrkB – in brain lysates and sections from WT and 5XFAD mice, ICV-injected either with PBS or with T cells, at 10 dpi. Fig. 3A shows that the baseline levels of both BDNF and TrkB were significantly reduced in hippocampal lysates

---

Fig. 1. Generation of Aβ-specific Th1 cells retrovirally transduced to overexpress and secrete a biologically active BDNF. (A) A scheme showing the generation of BDNF-producing, Aβ-specific Th1 cells. Two month-old mice were first vaccinated with Aβ1–42. After 7 d, CD4 T cells were purified from draining lymph nodes and stimulated with Aβ in the presence of antigen-presenting cells. The CD4 T cells were then polarized to a Th1 phenotype and transduced with the pMP71-EGFP-PRE and pMP71-BDNF-T2A-EGFP-PRE retroviruses to generate Th1-GFP and Th1-BDNF T cells, respectively. (B) Representative flow cytometry histograms showing EGFP mean fluorescence intensity (MFI) in Th1-GFP and Th1-BDNF T cells. (C) Secreted levels of BDNF measured by ELISA in supernatants of Th1-GFP and Th1-BDNF cells, 48 h after activation with anti-CD3/anti-CD28 Dynabeads. (D) WB analysis of BDNF expression in Th1-GFP and Th1-BDNF whole-cell lysates. Th1 cells producing GFP and BDNF were activated with anti-CD3/anti-CD28 Dynabeads and the cells were collected 48 h later. Recombinant BDNF (rBDNF) was used as a control. (E) Representative images of Th1-GFP and Th1-BDNF cells immunolabeled with anti-BDNF (red) and nuclei-labeled with DAPI (blue). (F) WB analysis of non-phosphorylated and phosphorylated TrkB (707/706) and ERK1/2 in lysates of HEK293T TrkB-transduced cells treated with Th1-GFP and Th1-BDNF cell supernatants (2.5 ng/ml BDNF) or with recombinant BDNF (rBDNF, 2.5 ng/ml) for 15, 30, 45, or 60 min, as indicated. Tubulin served as an internal loading control.
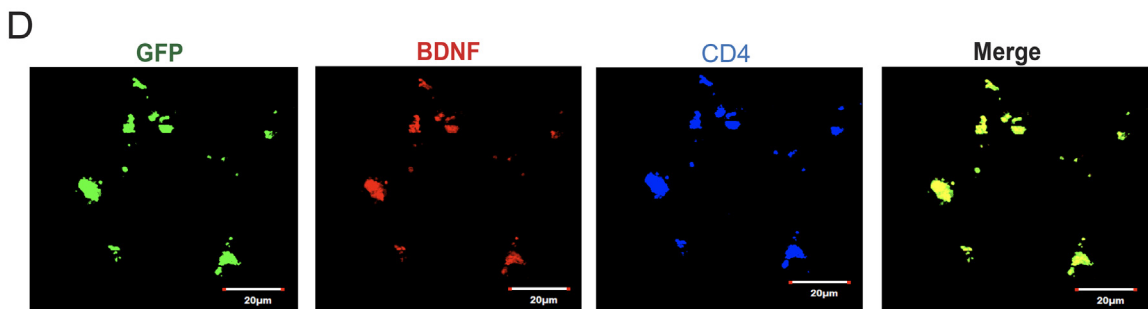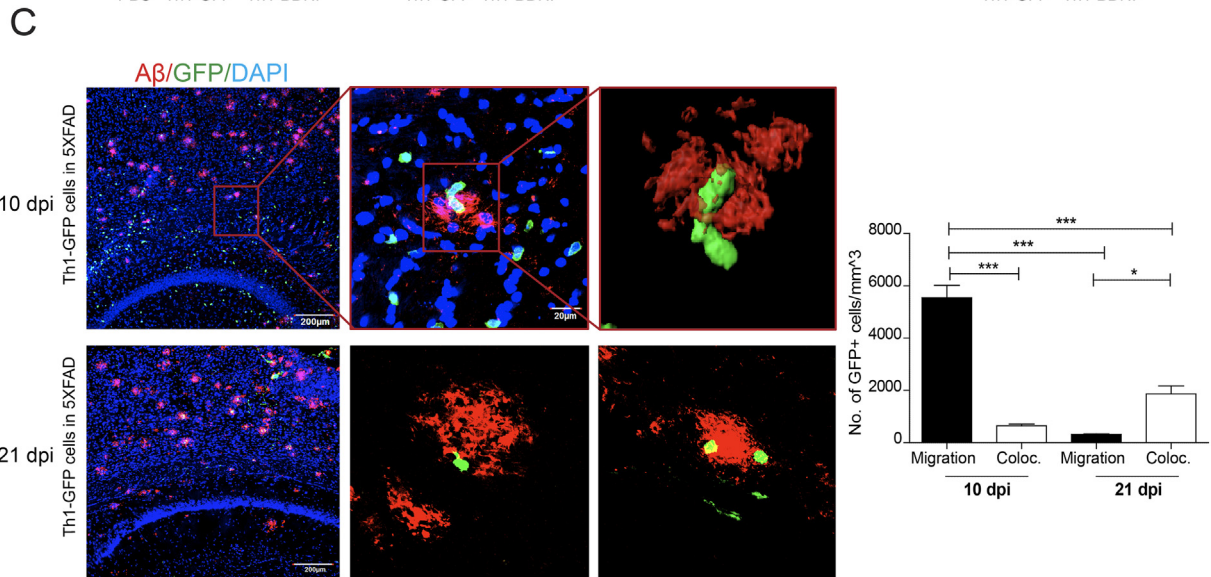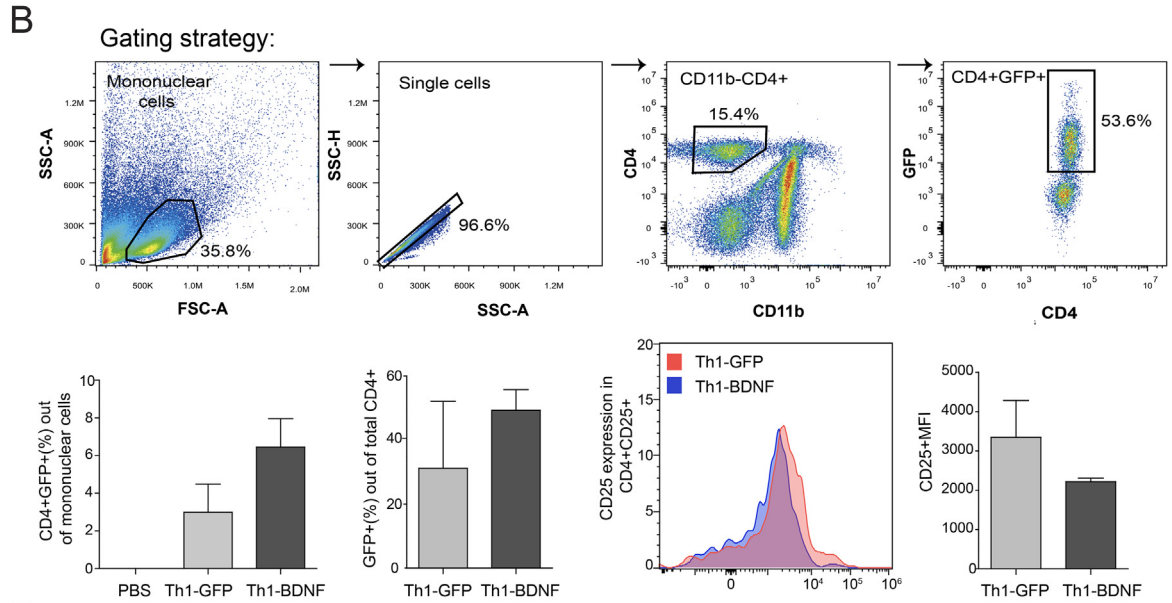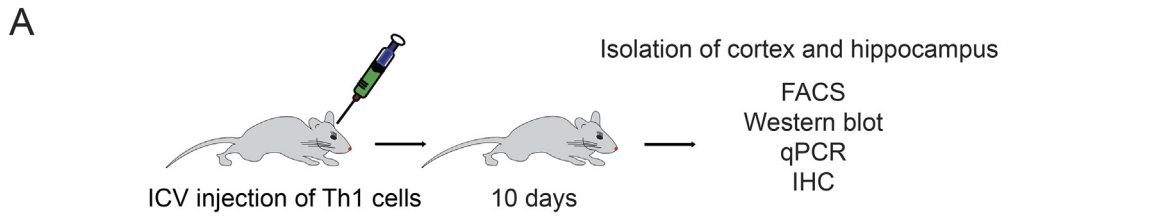
from 5XFAD (Fig. 3A), as compared with their levels in WT mice. Notably, 5XFAD mice ICV-injected with Th1-BDNF, but not with Th1-GFP cells, showed significantly higher levels of both BDNF and TrkB in the hippocampus (Fig. 3B). To determine whether Th1-BDNF cells induce TrkB phosphorylation, we performed IHC analysis of pTrkB in brain sections of 5XFAD mice ICV-injected with Th1-BDNF or Th1-GFP cells (Fig. 3C), and ICC analysis of pTrkB in primary neurons co-cultured with the T cells for 2 h (Fig. 3D). Recombinant BDNF was used as a positive control. In both experiments, Th1-BDNF cells increased the levels of pTrkB as compared with Th1-GFP cells. Notably, IHC analysis of BDNF in hippocampal sections of 5XFAD mice revealed that its increased levels observed in lysates from mice that were ICV-injected with Th1-BDNF cells was due, not only to its expression in T cells, but also due to its upregulation in dentate gyrus neurons (Supplementary Fig. 2).

Synaptic loss in the hippocampus is another key pathological hallmark of AD [21,22,42]. Such changes in both presynaptic (e.g., synaptophysin, SNAP25, and VAMP2) and postsynaptic (e.g., PSD-95) proteins were observed in various mouse models of AD [42–44]. Therefore, we performed a WB analysis to examine whether the ICV-injected Th1-GFP or Th1-BDNF cells affect the expression of synaptic molecules in the brain parenchyma. While PSD-95, SNAP25, VAMP2 and synaptophysin protein levels were not reduced in the hippocampus of 5XFAD compared with WT mice that were ICV-injected with PBS (Fig. 4A), they showed a trend of increased expression (with VAMP2 being significantly increased) in mice that were ICV-injected with Th1-BDNF, as compared with mice that were ICV-injected with Th1-GFP cells or with PBS (Fig. 4B). Both Th1-BDNF and Th1-GFP cells increased the levels of NeuN in the hippocampus, as compared with PBS (Fig. 4B). Overall, these findings suggest that ICV-injected Th1 T cells increase neuronal viability in the hippocampus and that the overexpression of BDNF by the cells further promotes synaptic and neuronal rescue.

3.4. ICV-injected Th1-BDNF cells ameliorate amyloid pathology in the cortex of 5XFAD mice

The generation of Aβ peptides by proteolytical processing of APP is mediated by the beta-site APP cleaving enzyme 1 (BACE1) and the gamma-secretase complex [17,45,46]. To examine whether Th1-BDNF or Th1-GFP cells affect amyloid pathology, we measured the levels of Aβ plaques in the cortex at 45 dpi. An IHC analysis of Aβ plaques showed that, as compared with PBS-injected mice, plaque pathology was significantly reduced in the cortex of 11–12-month old 5XFAD mice ICV-injected with either Th1-BDNF or Th1-GFP cells (Fig. 5A). This decrease was accompanied by increased levels of the phagocytic marker SIRP-β1 and reduced levels of the neurotoxic inflammatory cytokine IL-1β (Fig. 5B).

Finally, we examined whether, in addition to increased Aβ uptake, the T cells also affected the expression of BACE1 and APP in the brain of 5XFAD mice. A WB analysis of cortical lysates showed that the expression of both APP and BACE1 significantly increased in 11–12-month old 5XFAD mice, as compared with WT control mice that were ICV-injected with PBS (Fig. 5C–D). Conversely, when 5XFAD mice were ICV-injected with Th1-BDNF cells, but not with Th1-GFP cells or with PBS, the

expression levels of BACE1 in the brain were significantly reduced, whereas those of APP did not change (Fig. 5E-F).

4. Discussion

We present a novel T-cell based platform for the delivery of beneficial proteins to specific loci within the CNS. We show that Aβ-specific Th1 cells, genetically modified to secrete BDNF and ICV-injected into the 5XFAD mouse model of AD, effectively migrate to sites of Aβ plaques in the brain parenchyma, where they increase the levels of BDNF and its receptor TrkB. Furthermore, the injected Th1-BDNF T cells induced up-regulation of synaptic molecules and reduced amyloid load and the associated neurotoxic inflammation in the brain. Therefore, we demonstrate an Aβ-targeted drug-delivery system, based on the capacity of specific CD4 T cells to effectively migrate within the brain parenchyma, target amyloid plaques, and release their cargo.

An efficacious delivery of potential therapeutic proteins (such as BDNF) into the CNS requires that optimal doses of the proteins are released at specific anatomical regions where neuronal damage takes place. Cell-based delivery systems appear to be a promising approach due to the ability of cells to migrate within the CNS, reside in the tissue, and locally produce the protein of interest [4]. Previous studies employed fibroblasts [47] or neuronal stem cells [26] engrafted into the hippocampus as a cell-therapy approach for the delivery of BDNF into the CNS. Whereas these attempts resulted in neuronal repair and in recovery of behavioral deficits, the chemotaxis of the cells toward Aβ plaques was limited, and Aβ load remained unaffected [26]. Here, we demonstrate that an ICV injection of Aβ-specific CD4 T cells genetically engineered to express BDNF, not only target Aβ plaques in the brain, but also secretes a biologically active BDNF specifically in brain areas affected by Aβ.

The loss of synapses and neurons are key pathological features of AD [18,43,44,48,49] and may, at least in part, occur due to the reduced levels of BDNF and TrkB [36,50–53]. Notably, higher serum levels of BDNF are associated with a slower rate of cognitive decline in people with AD [54], and BDNF-based therapies markedly improve synaptic efficiency and plasticity [25,27,29,55]. Here, we demonstrate that Th1-BDNF T cells increased the levels of total TrkB and pTrkB in the hippocampus of 5XFAD mice, similar to previous observations using the TrkB agonist, 7,8-dihydroflavone [36]. pTrkB levels were also more pronounced in our study in primary hippocampal neurons co-cultured with Th1-BDNF than with Th1-GFP cells. Furthermore, our data demonstrate that the Th1-BDNF T cells increased the level of VAMP2 protein, one of the vesicle-associated membrane proteins involved in the fusion of pre-synaptic vesicles and neurotransmitter release [56], in the brain of 5XFAD mice. Whereas only the levels of VAMP2 were significantly increased following the treatment, other synaptic molecules, including synaptophysin, and SNAP25, showed a similar trend. Together with the increased expression of NeuN in the hippocampus, our data suggest that the ICV-injected CD4 T cells, specifically those genetically modified to express BDNF, can contribute to synaptic and neuronal repair. However, further studies are required to determine the role of BDNF-expressing T cells in rescuing neuronal function and cognitive decline in the context of AD-like pathology.

Our findings suggest that the ICV-injected Th1-BDNF cells affected the amyloidogenic process in the brain of 5XFAD mice. Previous studies

Fig. 2. Th1-BDNF cells ICV-injected into 5XFAD mice migrate to the brain parenchyma and target Aβ plaques. (A) Experimental scheme: 5XFAD mice were ICV-injected with Th1-GFP cells, Th1-BDNF cells, or PBS (n = 6–7 mice per group) and killed 10 d later. Their hippocampi and cortexes were then excised and analyzed by various methods, as indicated. (B) Representative flow cytometry plots from brain cells of 5XFAD mice gated on CD4+CD11b− cells and analyzed for GFP expression. Graphs (lower panels, left to right) show the percentage of GFP+CD4+ cells out of the brain mononuclear cells, percentage of GFP+ cells out of the total CD4+ cells in the brain, and CD25 MFI in the CD4+GFP+ cell population, in each experimental group. Bars represent means ± SEM. (C) Representative brain sections obtained from Th1-GFP → 5XFAD mice 10 and 21 dpi and immunolabeled with anti-Aβ (red) and DAPI (nuclei staining, blue). Images show the merge of Aβ, GFP+ cells (green) and DAPI. Right panel shows a 3D reconstruction of z-sections, demonstrating the co-localization of Th1-GFP cells (green) with an Aβ plaque (red). Graph represents the number of migrating GFP+ T cells and the degree of co-localization between GFP+ T cells and Aβ-plaques at 10 and 21 days post ICV injection. (D) Representative brain sections from 5XFAD mice that were ICV-injected with Th1-BDNF cells and immunolabeled with anti-BDNF (red) and anti-CD4 (blue) antibodies. Merged image shows GFP+ (green) cells colocalized with CD4 cells and BDNF.
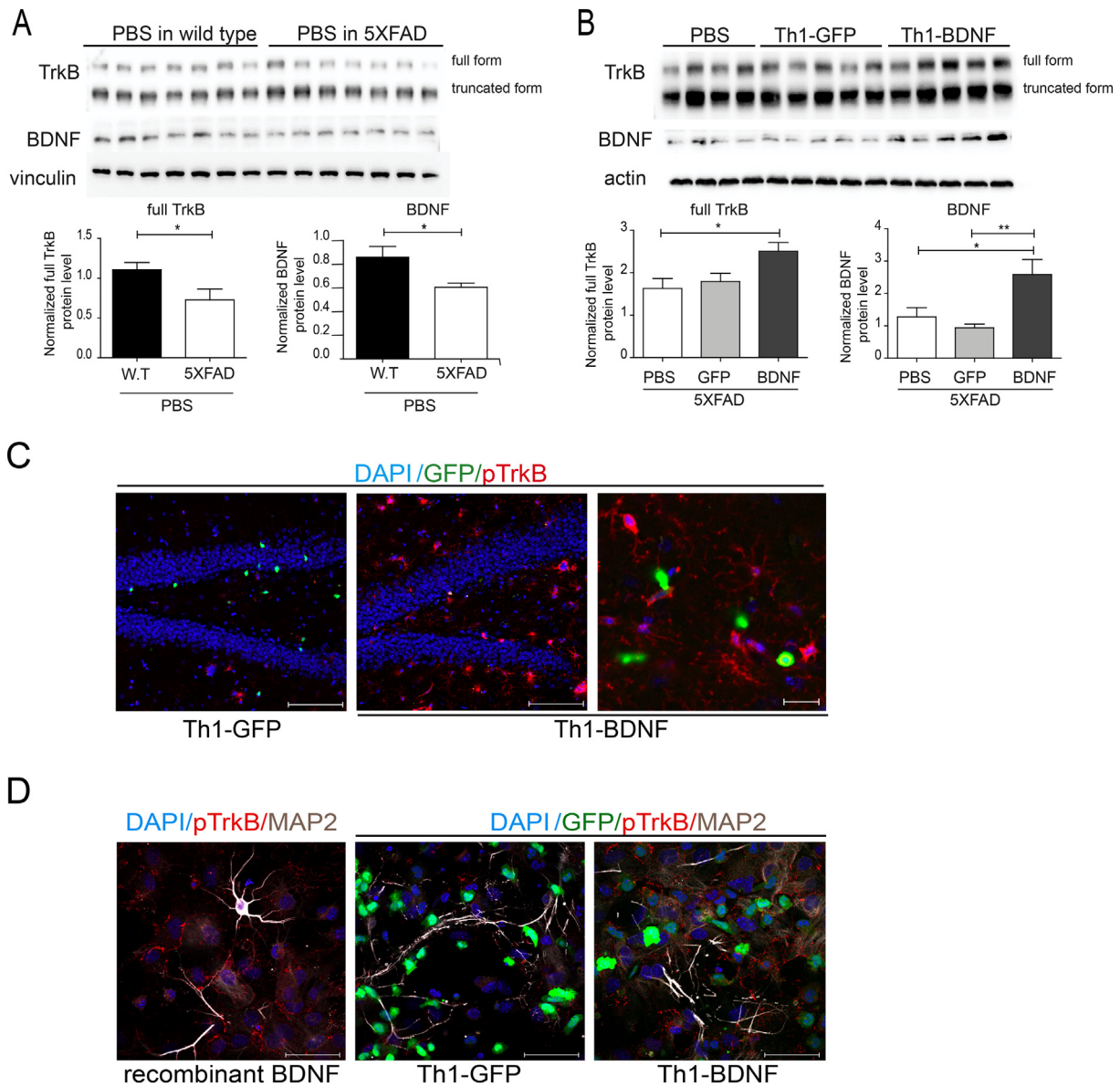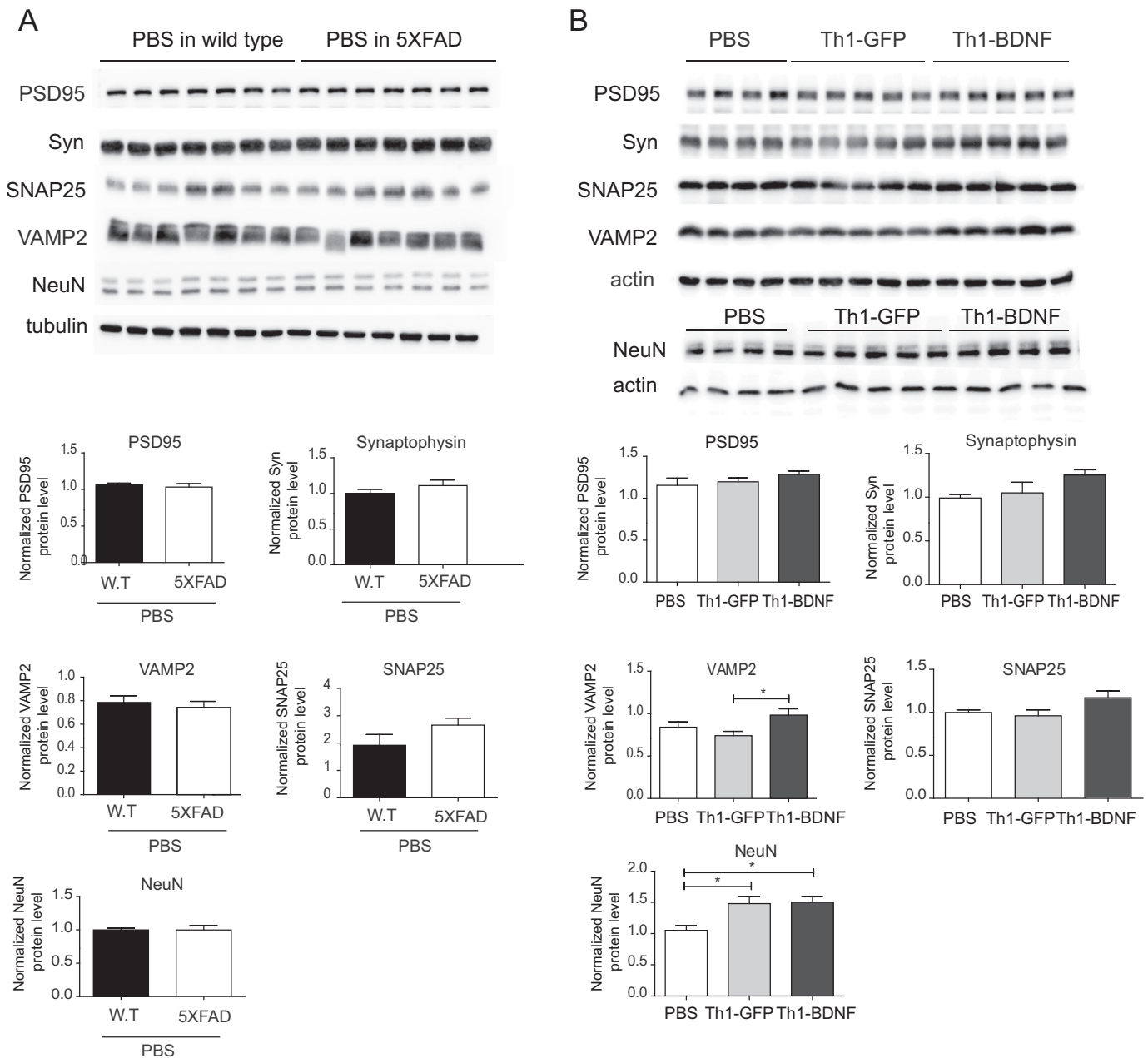
Fig. 3. Th1-BDNF cells facilitate TrkB signaling in 5XFAD mice and in primary neurons. 5XFAD mice (11–12 months old) were ICV-injected with Th1-GFP cells, Th1-BDNF cells, or PBS ($n =$ 6–7 mice per group). As an additional baseline control experiment, 5XFAD mice and littermate wild-type (WT) controls were injected with PBS ($n = 6$–7 mice per group). The mice were killed 10 d after the injection and their brains were excised and analyzed with WB and IHC. (A) WB analysis of TrkB and BDNF in whole hippocampal homogenates from WT and 5XFAD mice that were ICV-injected with PBS. Vinculin was used as an internal control. Bar graphs show the mean ($\pm$ SEM) levels of BDNF and TrkB normalized to those of vinculin in each lysate. $^*p < .05$ (Student's-t-test). (B) WB analysis of TrkB and BDNF in whole hippocampal homogenates from 5XFAD mice ICV-injected with Th1-GFP, Th1-BDNF, or PBS. Actin was used as an internal control. Bar graphs show the mean ($\pm$ SEM) levels of BDNF and TrkB normalized to those of actin in each lysate. $^*p < .05$, $^{**}p < .01$ (one-way ANOVA). (C) Representative brain sections obtained from 5XFAD mice ICV-injected with Th1-GFP (left panel) or Th1-BDNF cells (mid panel), immunolabeled with anti-pTrkB (red) and counterstained with DAPI (blue). Scale bars represent 50 μM. Right panel represents a higher resolution image from the hippocampus of a 5XFAD mouse, ICV-injected with Th1-BDNF cells. Scale bar represents 20 μM. (D) Representative images of primary hippocampal neurons immunolabeled with anti-pTrkB (red) and anti-MAP2 (white) and counterstained with DAPI (blue). Neurons (4×10^4 cells per well) were incubated with recombinant BDNF (100 ng/ml) for 15 min (left panel) or co-cultured with Th1-GFP (mid panel) or Th1-BDNF (right panel) cells (2×10^5) for 2 h. Scale bars represent 50 μm.

demonstrated that reducing the levels of BACE1, which cause increased production of Aβ in the brain parenchyma, has marked benefecial effects on the disease process [57–59]. Notably, the higher levels of BACE1 that we observed in the brains of 11–12-month old 5XFAD mice, as compared with its levels in age-matched WT controls, were lower in the Th1-BDNF-injected 5XFAD mice. Although both Th1-BDNF and Th1-GFP cells induced Aβ clearance—a function presumably related primarily to the enhanced phagocytic capacity of microglia [38,60]—BACE1 was downregulated only by Th1-BDNF cells such as previously observed following peripheral administration of a TrkB agonist to 5XFAD mice [36]. Further studies should unveil the role of BDNF in

regulating the expression of BACE1 and in the amyloidogenic process within the AD-affected brain.

Neurotoxic inflammation is considered a key factor in the progression of AD [19,20,23,61–64]. The progressive accumulation of misfolded proteins in the form of neurotoxic oligomers and plaques appears to play a role in the neurotoxic inflammatory response induced in the brain of people with AD [65,66]. The Aβ-specific Th1 cells that we used may thus boost adaptive immunity in the brain, which impacts not only the uptake of Aβ, but also the inflammatory reaction in the brain. Indeed, our findings show that both Th1-BDNF and Th1-GFP cells induced an upregulation of the phagocytic protein SIRPβ1 and
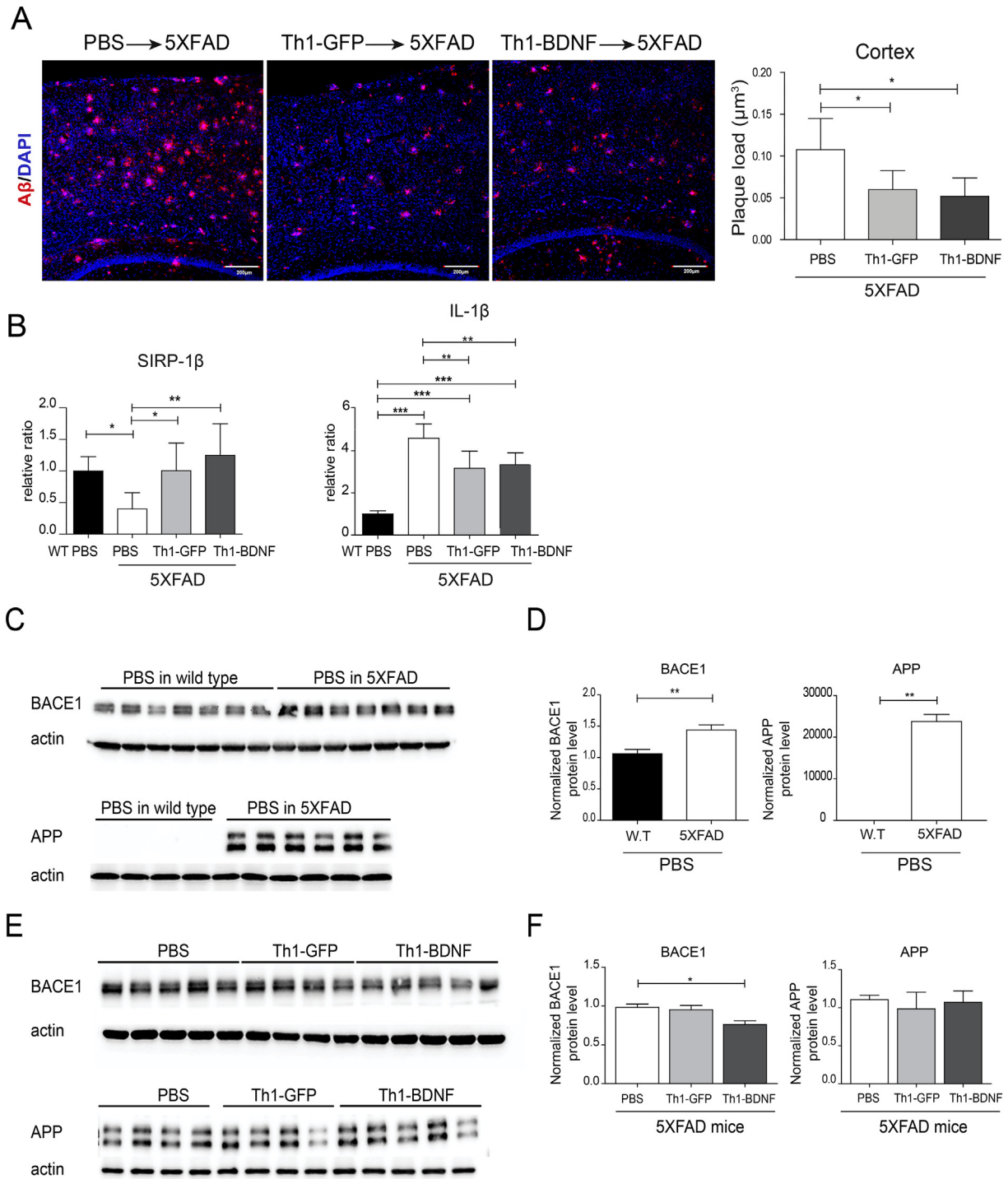
Fig. 4. Neuronal repair is induced in the hippocampus of 5XFAD mice ICV-injected with Th1-BDNF cells. 5XFAD mice (11–12 months old) were ICV-injected with Th1-GFP cells, Th1-BDNF cells, or PBS (*n* = 6–7 mice per group). As an additional baseline control experiment, 5XFAD mice and littermate WT controls were injected with PBS (n = 6–7 mice per group). The mice were killed 10 d following the injection and their brains were excised and analyzed with WB. (A) WB analysis of PSD95, synaptophysin (Syn), SNAP25, VAMP25, and NeuN in whole hippocampal homogenates from WT and 5XFAD mice ICV-injected with PBS. Tubulin was used as an internal control. Bar graphs indicate the mean (± SEM) levels of each protein, normalized to tubulin levels in each lysate. (B) WB analysis of the above-mentioned proteins in whole hippocampal homogenates from 5XFAD mice ICV-injected with Th1-GFP cells, Th1-BDNF cells, or PBS. Actin was used as an internal control. Bar graphs indicate the mean (± SEM) levels of PSD95 (*p* = .2852), synaptophysin (Syn) (*p* = .124), SNAP25 (*p* = .0939), VAMP25 and NeuN, normalized to actin levels for each lysate. *$p < .05$ (one-way ANOVA).

reduced the levels of IL-1β in the brain. In contrast to the almost dominant innate immune reaction evident in the AD brain [63,67–69], such antigen-specific T cells appear to achieve better control over the generation and clearance of misfolded proteins.

Several studies have provided promising evidence that an intrathecal or intravenous administration of stem cells can be used to treat multiple sclerosis [70–72] and amyotrophic lateral sclerosis [73]. Thus, an intrathecal administration of activated CD4 T cells to patients with AD appears to be clinically feasible. Whereas an intravenous administration appears to be advantageous over an intrathecal or ICV administration,

further research is required to ensure that the migration of cells to Aβ plaques in the brain is effective and does not cause neurotoxic vascular and/or parenchymal inflammation [74]. Finally, additional studies are required to optimize the therapeutic capacity of T cells (including, for instance, their phenotype, injection site, number of cells, and controlled drug release); their multifactorial impact in a disease setting in which the immune system is deteriorated [75–77] may be a promising strategy for the treatment of various neurodegenerative disorders.

Supplementary data to this article can be found online at https://doi.org/10.1016/j.ebiom.2019.04.019.

Fig. 5. ICV-injected Th1-GFP and Th1-BDNF cells ameliorate Aβ pathology in 5XFAD mice. 5XFAD mice (11–12 months old) were ICV-injected with Th1-GFP cells, Th1-BDNF cells, or PBS (n = 5–7 mice per group) WT type mice were ICV-injected with PBS. After 45 d, the mice were killed and their cortexes were analyzed using IHC, qPCR and WB. (A) Representative brain sections immunolabeled with anti-Aβ (red), counterstained with TO-PRO (blue), and analyzed with confocal microscopy for amyloid plaques. Right graph shows the mean (± SEM) of the Aβ plaque load per volume of section in the cortex (four sections per mouse in one representative experiment; n = 3–5). *p < .05 (one-way ANOVA). (B) RNA was extracted from the cortex of WT mice ICV-injected with PBS and of 5XFAD mice ICV-injected with PBS, Th1-GFP cells, or Th1-BDNF cells. Bar graphs represent mean (± SEM) levels of IL-1β and SIRP-1β mRNAs in the cortexes of these mice, analyzed using qPCR. *p < .05, **p < .01, ***p < .001 (one-way ANOVA). (C) WB analysis of BACE1 and APP in lysates from brain cortexes of 5XFAD and WT mice ICV-injected with PBS. Actin was used as an internal control. (D) Mean (± SEM) BACE1 and APP levels, normalized to actin levels, in each lysate. **p < .01 (Student's-t-test). (E) WB analysis of BACE1 and APP in lysates from cortexes of 5XFAD mice ICV-injected with PBS, Th1-GFP cells, or Th1-BDNF cells. Actin was used as an internal control. (F) Mean (± SEM) BACE1 and APP levels, normalized to actin levels, in each lysate. *p < .05 (one-way ANOVA).

References

[1] Batrakova EV, Gendelman HE, Kabanov AV. Cell-mediated drug delivery. Expert Opin Drug Deliv 2011;8(4):415–33.

[2] Upadhyay RK. Drug delivery systems, CNS protection, and the blood brain barrier. Biomed Res Int 2014;2014:869269.

[3] Makar TK, et al. Brain-derived neurotrophic factor (BDNF) gene delivery into the CNS using bone marrow cells as vehicles in mice. Neurosci Lett 2004;356(3): 215–9.

[4] Makar TK, et al. Cell-based delivery of brain-derived neurotrophic factor in experimental allergic encephalomyelitis. J Interferon Cytokine Res 2014;34(8): 641–7.

[5] Biju K, et al. Macrophage-mediated GDNF delivery protects against dopaminergic neurodegeneration: a therapeutic strategy for Parkinson's disease. Mol Ther 2010; 18(8):1536–44.

[6] Chen C, et al. GDNF-expressing macrophages mitigate loss of dopamine neurons and improve parkinsonian symptoms in MitoPark mice. Sci Rep 2018;8(1):5460.

[7] Bemelmans AP, et al. Lentiviral-mediated gene transfer of brain-derived neurotrophic factor is neuroprotective in a mouse model of neonatal excitotoxic challenge. J Neurosci Res 2006;83(1):50–60.

[8] Nagahara AH, et al. MR-guided delivery of AAV2-BDNF into the entorhinal cortex of non-human primates. Gene Ther 2018;25(2):104–14.

[9] Wong HL, Wu XY, Bendayan R. Nanotechnological advances for the delivery of CNS therapeutics. Adv Drug Deliv Rev 2012;64(7):686–700.

[10] Xing Y, et al. Non-viral liposome-mediated transfer of brain-derived neurotrophic factor across the blood-brain barrier. Neural Regen Res 2016;11(4):617–22.

[11] Limongi T, et al. Delivery of brain-derived neurotrophic factor by 3D biocompatible polymeric scaffolds for neural tissue engineering and neuronal regeneration. Mol Neurobiol 2018;55(12):8788–98.

[12] De Miranda BR, et al. Astrocyte-specific DJ-1 overexpression protects against rotenone-induced neurotoxicity in a rat model of Parkinson's disease. Neurobiol Dis 2018;115:101–14.

[13] Xuan AG, et al. BDNF improves the effects of neural stem cells on the rat model of Alzheimer's disease with unilateral lesion of fimbria-fornix. Neurosci Lett 2008; 440(3):331–5.

[14] Metcalfe SM, Bickerton S, Fahmy T. Neurodegenerative disease: a perspective on cell-based therapy in the new era of cell-free Nano-therapy. Curr Pharm Des 2017;23(5):776–83.

[15] Sinha S, Lieberburg I. Cellular mechanisms of beta-amyloid production and secretion. Proc Natl Acad Sci U S A 1999;96(20):11049–53.

[16] De Strooper B, Annaert W. Proteolytic processing and cell biological functions of the amyloid precursor protein. J Cell Sci 2000(113):1857–70 Pt 11.

[17] Chow VW, et al. Modeling an anti-amyloid combination therapy for Alzheimer's disease. Sci Transl Med 2010;2(13):13ra1.

[18] Koffie RM, Hyman BT, Spires-Jones TL. Alzheimer's disease: synapses gone cold. Mol Neurodegener 2011;6(1):63.

[19] Heneka MT, et al. Neuroinflammation in Alzheimer's disease. Lancet Neurol 2015;14 (4):388–405.

[20] Ardura-Fabregat A, et al. Targeting Neuroinflammation to treat Alzheimer's disease. CNS Drugs 2017;31(12):1057–82.

[21] Clare R, et al. Synapse loss in dementias. J Neurosci Res 2010;88(10):2083–90.

[22] Hamos JE, DeGennaro LJ, Drachman DA. Synaptic loss in Alzheimer's disease and other dementias. Neurology 1989;39(3):355–61.

[23] Heppner FL, Ransohoff RM, Becher B. Immune attack: the role of inflammation in Alzheimer disease. Nat Rev Neurosci 2015;16(6):358–72.

[24] Phillips HS, et al. BDNF mRNA is decreased in the hippocampus of individuals with Alzheimer's disease. Neuron 1991;7(5):695–702.

[25] Murer MG, Yan Q, Raisman-Vozari R. Brain-derived neurotrophic factor in the control human brain, and in Alzheimer's disease and Parkinson's disease. Prog Neurobiol 2001;63(1):71–124.

[26] Blurton-Jones M, et al. Neural stem cells improve cognition via BDNF in a transgenic model of Alzheimer disease. Proc Natl Acad Sci U S A 2009;106(32):13594–9.

[27] Budni J, et al. The involvement of BDNF, NGF and GDNF in aging and Alzheimer's disease. Aging Dis 2015;6(5):331–41.

[28] Pardridge WM. Alzheimer's disease drug development and the problem of the blood-brain barrier. Alzheimers Dement 2009;5(5):427–32.

[29] Nagahara AH, Tuszynski MH. Potential therapeutic uses of BDNF in neurological and psychiatric disorders. Nat Rev Drug Discov 2011;10(3):209–19.

[30] Connor B, et al. Brain-derived neurotrophic factor is reduced in Alzheimer's disease. Brain Res Mol Brain Res 1997;49(1–2):71–81.

[31] Hock C, et al. Region-specific neurotrophin imbalances in Alzheimer disease: decreased levels of brain-derived neurotrophic factor and increased levels of nerve growth factor in hippocampus and cortical areas. Arch Neurol 2000;57(6):846–51.

[32] Michalski B, Fahnestock M. Pro-brain-derived neurotrophic factor is decreased in parietal cortex in Alzheimer's disease. Brain Res Mol Brain Res 2003;111(1–2):148–54.

[33] Peng S, et al. Precursor form of brain-derived neurotrophic factor and mature brain-derived neurotrophic factor are decreased in the pre-clinical stages of Alzheimer's disease. J Neurochem 2005;93(6):1412–21.

[34] Ginsberg SD, et al. Microarray analysis of hippocampal CA1 neurons implicates early endosomal dysfunction during Alzheimer's disease progression. Biol Psychiatry 2010;68(10):885–93.

[35] Peng S, et al. Decreased brain-derived neurotrophic factor depends on amyloid aggregation state in transgenic mouse models of Alzheimer's disease. J Neurosci 2009;29(29):9321–9.

[36] Devi L, Ohno M. 7,8-dihydroxyflavone, a small-molecule TrkB agonist, reverses memory deficits and BACE1 elevation in a mouse model of Alzheimer's disease. Neuropsychopharmacology 2012;37(2):434–44.

[37] Ma XC, et al. Intranasal delivery of recombinant AAV containing BDNF fused with HA2TAT: a potential promising therapy strategy for major depressive disorder. Sci Rep 2016;6:22404.

[38] Fisher Y, et al. Th1 polarization of T cells injected into the cerebrospinal fluid induces brain immunosurveillance. J Immunol 2014;192(1):92–102.

[39] Engels B, et al. Retroviral vectors for high-level transgene expression in T lymphocytes. Hum Gene Ther 2003;14(12):1155–68.

[40] Andreska T, et al. High abundance of BDNF within glutamatergic presynapses of cultured hippocampal neurons. Front Cell Neurosci 2014;8:107.

[41] Lee J, et al. Decreased levels of BDNF protein in Alzheimer temporal cortex are independent of BDNF polymorphisms. Exp Neurol 2005;194(1):91–6.

[42] Oakley H, et al. Intraneuronal beta-amyloid aggregates, neurodegeneration, and neuron loss in transgenic mice with five familial Alzheimer's disease mutations: potential factors in amyloid plaque formation. J Neurosci 2006;26(40):10129–40.

[43] Shao CY, et al. Postsynaptic degeneration as revealed by PSD-95 reduction occurs after advanced Abeta and tau pathology in transgenic mouse models of Alzheimer's disease. Acta Neuropathol 2011;122(3):285–92.

[44] Harwell CS, Coleman MP. Synaptophysin depletion and intraneuronal Abeta in organotypic hippocampal slice cultures from huAPP transgenic mice. Mol Neurodegener 2016;11(1):44.

[45] Rossner S, et al. Alzheimer's disease beta-secretase BACE1 is not a neuron-specific enzyme. J Neurochem 2005;92(2):226–34.

[46] Ballard C, et al. Alzheimer's disease. Lancet 2011;377(9770):1019–31.

[47] Lucidi-Phillipi CA, et al. Brain-derived neurotrophic factor-transduced fibroblasts: production of BDNF and effects of grafting to the adult rat brain. J Comp Neurol 1995;354(3):361–76.

[48] Scheff SW, et al. Hippocampal synaptic loss in early Alzheimer's disease and mild cognitive impairment. Neurobiol Aging 2006;27(10):1372–84.

[49] Greber S, et al. Decreased levels of synaptosomal associated protein 25 in the brain of patients with down syndrome and Alzheimer's disease. Electrophoresis 1999;20 (4–5):928–34.

[50] Kowianski P, et al. BDNF: A Key Factor with Multipotent Impact on Brain Signaling and Synaptic Plasticity. Cell Mol Neurobiol 2018;38(3):579–93.

[51] Jia JM, et al. Brain-derived neurotrophic factor-tropomyosin-related kinase B signaling contributes to activity-dependent changes in synaptic proteins. J Biol Chem 2008;283(30):21242–50.

[52] Liao L, et al. BDNF induces widespread changes in synaptic protein content and up-regulates components of the translation machinery: an analysis using high-throughput proteomics. J Proteome Res 2007;6(3):1059–71.

[53] Ferrer I, et al. BDNF and full-length and truncated TrkB expression in Alzheimer disease. Implications in therapeutic strategies. J Neuropathol Exp Neurol 1999;58(7):729–39.

[54] Laske C, et al. Higher BDNF serum levels predict slower cognitive decline in Alzheimer's disease patients. Int J Neuropsychopharmacol 2011;14(3):399–404.

[55] Nagahara AH, et al. Neuroprotective effects of brain-derived neurotrophic factor in rodent and primate models of Alzheimer's disease. Nat Med 2009;15(3):331–7.

[56] Koo SJ, et al. Vesicular synaptobrevin/VAMP2 levels guarded by AP180 control efficient neurotransmission. Neuron 2015;88(2):330–44.

[57] Devi L, Ohno M. Genetic reductions of beta-site amyloid precursor protein-cleaving enzyme 1 and amyloid-beta ameliorate impairment of conditioned taste aversion memory in 5XFAD Alzheimer's disease model mice. Eur J Neurosci 2010;31(1):110–8.

[58] Devi L, Ohno M. Phospho-eIF2alpha level is important for determining abilities of BACE1 reduction to rescue cholinergic neurodegeneration and memory defects in 5XFAD mice. PLoS One 2010;5(9):e12974.

[59] Ohno M, et al. BACE1 gene deletion prevents neuron loss and memory deficits in 5XFAD APP/PS1 transgenic mice. Neurobiol Dis 2007;26(1):134–45.

[60] Schroder K, et al. Interferon-gamma: an overview of signals, mechanisms and functions. J Leukoc Biol 2004;75(2):163–89.

[61] Cao W, Zheng H. Peripheral immune system in aging and Alzheimer's disease. Mol Neurodegener 2018;13(1):51.

[62] Regen F, et al. Neuroinflammation and Alzheimer's disease: implications for microglial activation. Curr Alzheimer Res 2017;14(11):1140–8.

[63] Andreasson KI, et al. Targeting innate immunity for neurodegenerative disorders of the central nervous system. J Neurochem 2016;138(5):653–93.

[64] Baron R, et al. Accelerated microglial pathology is associated with Abeta plaques in mouse models of Alzheimer's disease. Aging Cell 2014;13(4):584–95.

[65] Wang YH, Zhang YG. Amyloid and immune homeostasis. Immunobiology 2018;223 (3):288–93.

[66] Selkoe DJ. Alzheimer's disease. Cold Spring Harb Perspect Biol 2011(3):7.

[67] Ransohoff RM, et al. Neuroinflammation: ways in which the immune system affects the brain. Neurotherapeutics 2015;12(4):896–909.

[68] Boutajangout A, Wisniewski T. The innate immune system in Alzheimer's disease. Int J Cell Biol 2013;2013:576383.

[69] Ransohoff RM, Brown MA. Innate immunity in the central nervous system. J Clin Invest 2012;122(4):1164–71.

[70] Scolding NJ, et al. Cell-based therapeutic strategies for multiple sclerosis. Brain 2017; 140(11):2776–96.

[71] Karussis D, Petrou P, Kassis I. Clinical experience with stem cells and other cell therapies in neurological diseases. J Neurol Sci 2013;324(1–2):1–9.

[72] Karussis D, et al. Hematopoietic stem cell transplantation in multiple sclerosis. Expert Rev Neurother 2013;13(5):567–78.

[73] Petrou P, et al. Safety and clinical effects of mesenchymal stem cells secreting neurotrophic factor transplantation in patients with amyotrophic lateral sclerosis: results of phase 1/2 and 2a clinical trials. JAMA Neurol 2016;73(3):337–44.

[74] Monsonego A, et al. Abeta-induced meningoencephalitis is IFN-gamma-dependent and is associated with T cell-dependent clearance of Abeta in a mouse model of Alzheimer's disease. Proc Natl Acad Sci U S A 2006;103(13):5048–53.

[75] Nikolich-Zugich J. The twilight of immunity: emerging concepts in aging of the immune system. Nat Immunol 2018;19(1):10–9.

[76] Goronzy JJ, Weyand CM. Understanding immunosenescence to improve responses to vaccines. Nat Immunol 2013;14(5):428–36.

[77] Montecino-Rodriguez E, Berent-Maoz B, Dorshkind K. Causes, consequences, and reversal of immune system aging. J Clin Invest 2013;123(3):958–65.